Hindawi
Geofluids
Volume 2021, Article ID 4673152, 13 pages
https://doi.org/10.1155/2021/4673152

*Research Article*

# Research on Optimization of Coal Pressure Relief Borehole Parameters under High-Stress Conditions

**Heng Zhang**,[1] **Tie Li**,[1] **Zhenhua Ouyang**,[2] **Su Liu**,[3] **and Haiyang Yi**[2]

[1]*School of Civil and Resource Engineering, University of Science and Technology Beijing, Beijing 100083, China*
[2]*School of Safety Regulation, North China Institute of Science and Technology, Hebei 065201, China*
[3]*School of Resources and Civil Engineering, Northeastern University, Shengyang 110819, China*

Correspondence should be addressed to Tie Li; litie@ustb.edu.cn

Received 17 June 2021; Revised 23 July 2021; Accepted 17 August 2021; Published 1 September 2021

Academic Editor: Zhijie Wen



Determining the parameters of boreholes drilled for relieving pressure in coal seams is the key preventing and controlling rock bursts in boreholes of large diameter. In this study, theoretical analysis, numerical simulation, literature research, and other analysis methods are applied to study the angles of elastic energy dissipation and stress transfer, the distribution law of the pressure relief area, and the areas of stress concentration, energy, stress, displacement, and plastic behavior of large-diameter pressure relief boreholes in coal seams under high-stress conditions. The results are then used to evaluate the relationship between large-diameter pressure relief boreholes and the borehole arrangement. The following results are obtained. (1) A large-diameter results in a large amount of elastic energy released by the surrounding coal, low residual elastic energy density, strong interaction between boreholes, large pressure relief range of the borehole, and high pressure relief efficiency. (2) The main evaluation factor of the borehole pressure relief effect is its thickness and stress concentration area; secondary evaluation is based on the areas of energy, displacement, stress, and plastic behavior. (3) Six evaluation index systems are established to evaluate the effects of borehole pressure relief, which are found to be the thicknesses of the borehole pressure relief area and stress concentration area, reduction degree of energy density, percentage of stress reduction, displacement, and penetration degree of the plastic area. (4) It is determined that when the diameters of the pressure relief boreholes are 100, 120, 180, and 200 mm, a single-row borehole arrangement is adopted; a three-pattern borehole arrangement is adopted with diameters of 140 and 160 mm. These research results can provide theoretical support in selecting reasonable borehole arrangements for pressure relief boreholes of different diameters.

## 1. Introduction

With the increases in coal mining depths in recent years, frequent mine rock burst accidents in coal mines have become major disasters [1–4]. However, large-diameter boreholes drilled in coal seams can effectively relieve the pressure on the seams, thus reducing the occurrence of rock burst accidents [5–8]. Many factors can affect the pressure relief function of boreholes such as mining technology geological factors, hole depth, and borehole aperture [9–11]. For a specific coal seam, considering the small fluctuation of geological factors such as coal seam strength and burial depth, mining technology factors such as mining height and mining method are basically fixed; only the borehole arrangement, angle, depth, diameter, spacing, and other physical factors can be changed. Therefore, determining reasonable borehole parameters for coal pressure relief is the key for preventing rock burst accidents.

Many scholars at home and abroad have conducted abundant research on coal pressure relief boreholes. Li et al. [12] studied the influencing factors of pressure relief boreholes in a high-stress coal roadway and showed that the borehole diameter, spacing, and depth jointly affect the pressure relief effect of the borehole. The research results of Geng et al. [13] showed that the arrangement of pressure relief boreholes has a certain influence on the pressure relief effect and that the effects vary with the borehole arrangement. The research results of LAN [14] showed improved

pressure relief effects of boreholes in high-stress areas of coal seams over those in low-stress areas. Jia et al. [15] studied the influence of borehole spacing, diameter, and depth on the strength of samples through laboratory tests and numerical analysis and found that stress release caused by crack propagation and penetration is fundamental for pressure relief in boreholes, with a larger borehole diameter, deeper depth, and smaller spacing showing better pressure relief effects. Yi et al. [16] studied and analyzed the pressure relief effects of large-diameter boreholes in soft and hard coal seams through numerical simulation, with better effects shown in the soft seams. Wang et al. [17] used stress transfer and surrounding rock deformation control effects as direct evaluation indices of the borehole pressure relief effect, categorizing the degree of borehole pressure relief as insufficient, sufficient, or excessive. Then, the dynamic action laws of length, diameter, and spacing of the pressure relief boreholes were applied to determine the stability of rocks surrounding a deep roadway. On the basis of the results, a method for determining the key parameters affecting the pressure relief was proposed. Liu et al. [18] and Zhang et al. [19] used numerical simulation based on Fast Lagrangian Analysis of Continua in Three Dimensions (FLAC3D) to determine that the peak stress of a coal seam can be transferred to deep areas by optimizing the borehole arrangement parameters. Qin [20] studied the stress, energy, and impact tendencies of coal and concluded that the pressure relief effect of large-diameter boreholes can be improved by adjusting the pressure of the coal, dissipating the energy, and reducing the impact properties. Li and Xiong[21] used automatic dynamic incremental nonlinear analysis, ADINA finite element analysis software, to study and evaluate the pressure relief effects of boreholes in stress concentration areas of rock bursts. Zhu et al. [22] put forward a concept based on the energy dissipation index, from which they deduced a quantitative calculation method of antiscour borehole parameters. Shi et al. [23] applied the Mohr strength theory and FLAC3D and determine that varying the borehole spacing and arrangement can significantly reduce large energy vibration occurring in rocks surrounding roadway to greatly reduce the impact risk of coal seams. Li et al. [24] studied the characteristics of the abutment pressure distribution, design scheme of the pressure relief borehole depth, and pressure relief effects in a large coal pillar after mining was conducted on a working face. On the basis of the results, a method was proposed for resolving the dangerous conditions of large coal pillars by controlling the depth and density of the pressure relief borehole, which enabled the transformation of stress distribution in the pillar from "single peak" to "ladle-shaped." Wang et al. [25] studied the effect of borehole pressure relief from the perspective of energy. Zhai et al. [26] considered that pressure relieved by large-diameter borehole is more effective for stress relief in large areas. Li et al. [27] put forward a method or evaluating pressure relief effects based on the tensile strain value of optical fiber and the pressure relief radius. In their study, the pressure relief process in the borehole was divided into four stages: fracture development, limit equilibrium, hole collapse, and crushing coal compaction. Zhang et al. [28] considered that a greater borehole density results in more energy released from the coal seam and thus better pressure relief effects of the borehole. Ge at al. [29] studied the relationship between different coal strengths and the spacing of pressure relief boreholes and put forth a formula based on the results.

Although such studies on pressure relief boreholes of large diameter in coal bodies are abundant, reasonable arrangement of pressure relief boreholes of various diameters under high-stress conditions has been studied less often. Thus, the present study uses the angles of energy dissipation and stress to evaluate the pressure relief effects of single-row, triple-flower, and double-row borehole arrangement schemes for pressure relief boreholes with varied diameters. The results are then applied to obtain the relationship between the borehole diameter and the arrangement mode. This research will provide certain theoretical support for pressure relief technology of large-diameter boreholes.

## 2. Mechanism Analysis

*2.1. Stress Transfer Mechanism of Pressure Relief Borehole.* Pressure relief using large-diameter boreholes is an effective measure for eliminating or reducing the risk of rock burst. After a pressure relief borehole is constructed in coal seam, the stress of the coal seams near the borehole is evaluated. By applying elastic-plastic theoretical analysis, an equation for such stress can be obtained [15, 30]:

$$\begin{cases} \sigma_x = \delta\left(1 - \dfrac{r^2}{l^2}\right), \\ \sigma_y = \delta\left(1 + \dfrac{r^2}{l^2}\right), \\ \tau = 0. \end{cases} \tag{1}$$

Radius of plastic zone $R_S$ [15, 30]:

$$R_S = r\left[\frac{l + c\cot\varphi}{c\cot\varphi}(1 - \sin\varphi)\right]^{(1-\sin\varphi)/(2\sin\varphi)}. \tag{2}$$

In these equations, $\sigma_x$, $\sigma_y$, $\tau$, and $\delta$ are the radial, tangential, shear, and original rock stresses near the borehole, respectively (units: MPa); $r$ is the borehole radius (m); $l$ is the distance between the coal and the borehole center (m); $R_S$ is the radius of the plastic zone (m); $c$ is cohesion in the coal (MPa); and $\varphi$ is the friction angle in the coal (MPa).

According to Equations (1) and (2), the stress around the borehole is redistributed from the original three-way stress state to the one-way stress state after the pressure relief borehole is arranged in the coal. When the stress of the coal is greater than its uniaxial compressive strength, the coal will be destroyed, and a plastic zone will appear around the borehole. The stress near the borehole is then transferred to a more distant location to form a new high-stress concentration area, and the elastic energy is accumulated locally in the plastic zone radius $R_S$ to form an elastic-plastic region.

With the increase in distance between the coal and the borehole, the stress state of the coal gradually returns to the original rock stress state (as shown in Figure 1).

After the construction of the large-diameter pressure relief borehole in high-stress coal, a new free surface is essentially created on the surface of borehole. The original rock stress at the free surface of the coal changes, and the stress in the area close to the borehole is released. The coal near the borehole contains cracks, and a broken area much larger in diameter than that of the borehole itself is created. When multiple boreholes are continually constructed in the coal, the broken areas connect, resulting in complete fracture of the rock mass along the borehole section. Then, the high-stress concentration area of the surrounding rock support is transferred to deep regions to achieve pressure relief (as shown in Figure 2). The crushing area changes the stress state of the coal seam, which reduces the ability of the coal seam to store destructive energy destructive energy and thus reduces the possibility of rock burst.

*2.2. Energy Dissipation Mechanism of Pressure Relief Borehole.* A coal unit in a rock mass deformed by external force was selected as the research object of the present study. Assuming that the activity was closed, i.e., the object did not exchange heat with the outside components, the total work performed by the external force is converted into energy $U$ according to the first law of thermodynamics [31].

$$U = U_j + U_\theta. \tag{3}$$

In this equation, $U_j$ is the dissipated energy of the element, and $U_\theta$ is the elastic strain energy of the element that can be released.

$$U = \int_0^{\varepsilon_1} \sigma_1 d\varepsilon_1 + \int_0^{\varepsilon_2} \sigma_2 d\varepsilon_2 + \int_0^{\varepsilon_3} \sigma_3 d\varepsilon_3, \tag{4}$$

$$U_j = \frac{1}{2}\sigma_1\varepsilon_1^e + \frac{1}{2}\sigma_2\varepsilon_2^e + \frac{1}{2}\sigma_3\varepsilon_3^e, \tag{5}$$

$$\varepsilon_i^e = \frac{1}{E_i}\left[\sigma_i - \nu_i\left(\sigma_j + \sigma_k\right)\right]. \tag{6}$$

In Equations (4)–(6), $\varepsilon_i$, $\varepsilon_i^e$, $E_i$, and $\nu_i$ are the total strain, total elastic strain, elastic modulus, and Poisson's ratio of the three principal stresses, respectively.

Assuming that the coal is an isotropic medium and that the initial values of $E_i$ and $\nu_i$ in the three principal stress directions are $E_0$ and $\nu_0$, respectively, Equations (5) and (6) can be obtained, and the elastic strain energy can be released by the coal unit [32].

$$U_j = \frac{1}{2E_0}\left[\sigma_1^2 + \sigma_2^2 + \sigma_3^2 - 2\nu_0\left(\sigma_1\sigma_2 + \sigma_1\sigma_3 + \sigma_2\sigma_3\right)\right]. \tag{7}$$

The change process of coal mechanics is essentially the process of energy dissipation, and that of coal instability is the rapid release process of accumulated elastic strain energy. When the accumulated energy of the coal unit is greater than its ultimate elastic energy, the coal unit will fracture. In the case of fixed coal occurrence and technical mining conditions, a greater amount of elastic strain energy of the coal unit released by the large-diameter pressure relief borehole is related to lower residual elastic strain energy, lower impact risk, and lower possibility of rock burst. Therefore, the effect of borehole pressure relief can be evaluated by the amount of elastic strain energy consumed by the large-diameter pressure relief borehole.

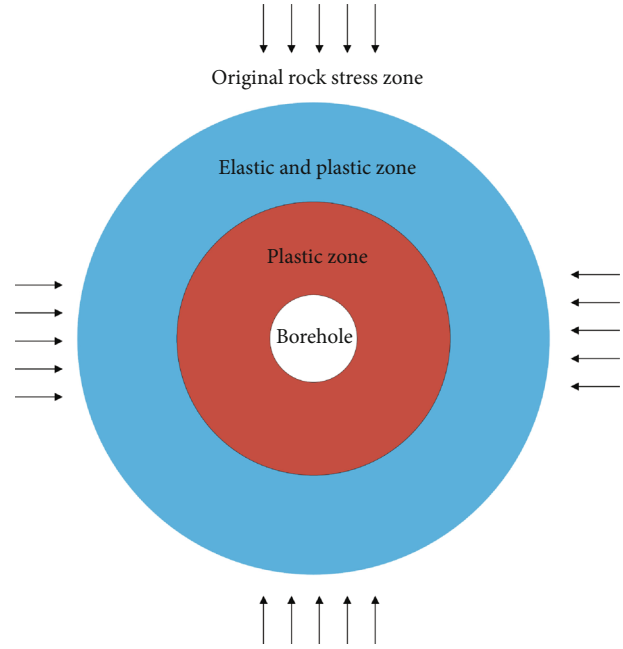


Figure 1: Elastic-plastic zone and stress distribution around a single borehole.

To study the energy release problem of large-diameter pressure relief boreholes in a coal unit, numerical simulation software can be used to calculate the local energy release rate of the coal unit and its elastic release energy [33].

$$\mathrm{LERR}_j = U_{j\,\max} - U_{j\,\min}, \tag{8}$$

$$\mathrm{ERE}_j = \sum_j^m \left(\mathrm{LERR}_j V_j\right). \tag{9}$$

In the above equation, $\mathrm{LERR}_j$ is the local energy release rate of the $j$th coal unit, $U_{j\,\max}$ is the peak elastic strain energy density prior to breakage of the coal of the $j$th unit, $U_{j\,\min}$ is the valley value of the elastic strain energy density of the $j$th coal unit after fracturing, $\mathrm{ERE}_j$ is the elastic strain energy released by the coal unit, and $V_j$ is the volume of the coal seams in unit $J$.

From Equation (7), the following can be concluded.

$$U_{j\,\max} = \frac{1}{2E_0}\left[\sigma_{j1}^2 + \sigma_{j2}^2 + \sigma_{j3}^2 - 2\nu_0\left(\sigma_{j1}\sigma_{j2} + \sigma_{j1}\sigma_{j3} + \sigma_{j2}\sigma_{j3}\right)\right], \tag{10}$$

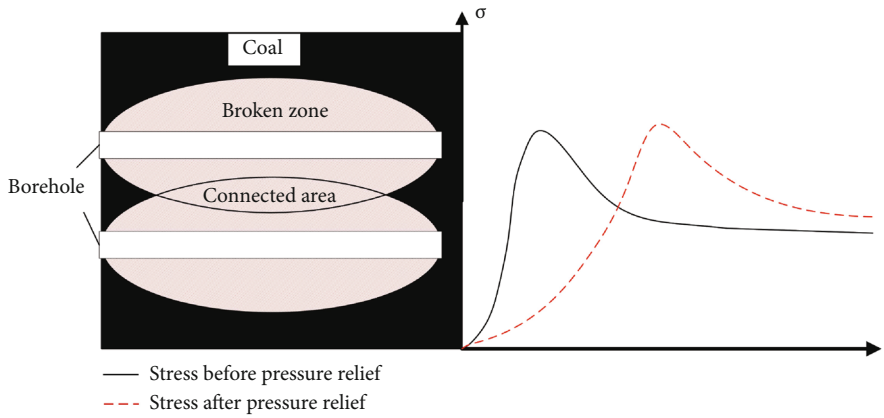


Figure 2: Diagram showing pressure relief in coal borehole.

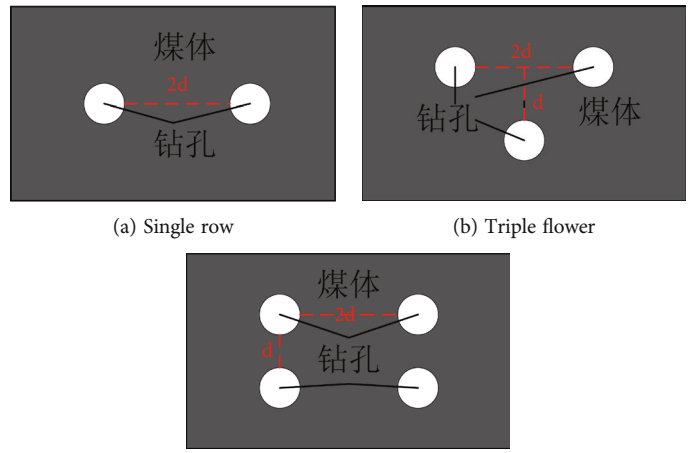


(a) Single row

(b) Triple flower

(c) Double row

Figure 3: Different borehole arrangements.

$$U_{j\,\min} = \frac{1}{2E_0}\left[\sigma_{j1'}^2 + \sigma_{j2'}^2 + \sigma_{j3'}^2 - 2v_0\left(\sigma_{j1'}\sigma_{j2'} + \sigma_{j1'}\sigma_{j3'} + \sigma_{j2'}\sigma_{j3'}\right)\right]. \tag{11}$$

In Equations (4)–(6), $\sigma_{j1}$, $\sigma_{j2}$, and $\sigma_{j3}$ are the principal stresses in three directions at the peak elastic strain energy density of the coal element, and $\sigma_{j1'}$, $\sigma_{j2'}$, and $\sigma_{j3'}$ are those at the valley value.

## 3. Numerical Simulation Scheme and Results

*3.1. Modeling and Scheme.* To study the different diameters of pressure relief boreholes and to determine the most effective type of borehole arrangement, the Mohr Coulomb model was established by using FLAC3D numerical simulation software. Six types of pressure relief boreholes of varied diameters were selected, and each group of pressure relief borehole was divided into single-row, triple-flower, or and double-row type. The detailed arrangement is shown in Figure 3, with panel (d) showing the borehole spacing. In total, 18 groups of models were used; their size, number of units, number of nodes, and other parameters are shown in Table 1. The top of the model was subjected to a high stress of 45 MPa; the bottom and surrounding parts of the model were fixed; and the top was in free-boundary condition. The mechanical parameters of the coal are shown in Table 2.

*3.2. Results Analysis*

*3.2.1. Arrangement of Single-Diameter Pressure Relief Borehole.* The pressure relief borehole of 140 mm in diameter was used as an example for analyzing the thicknesses of the zones of pressure relief, stress concentration, energy density, stress, strain, and plastic behavior near the borehole under the arrangements of single-row, triple-flower, and double-row boreholes. On the basis of the results, the optimal borehole arrangement was obtained.

*(1) Thicknesses of Borehole Pressure Relief and Stress Concentration Areas.* Figure 4 shows the thickness distribution of the pressure relief and stress concentration areas under different borehole arrangements. The thicknesses of the two areas are closely related to the borehole. Therefore, the thicknesses of the pressure relief area and the stress concentration

Table 1: Parameters of numerical calculation model.

| Serial number | Borehole diameter | Borehole arrangement | Model size/M | Number of units | Number of nodes |
|---|---|---|---|---|---|
| 1 | 100 mm | Single row | 2.3 ∗ 0.5 ∗ 3 | 15360 | 23763 |
| 2 | 100 mm | Triple flower | 2.5 ∗ 0.5 ∗ 3 | 18240 | 28197 |
| 3 | 100 mm | Double row | 2.5 ∗ 0.5 ∗ 3 | 17920 | 27231 |
| 4 | 120 mm | Single row | 2.36 ∗ 0.5 ∗ 3 | 16340 | 24856 |
| 5 | 120 mm | Triple flower | 2.6 ∗ 0.5 ∗ 3 | 18240 | 28917 |
| 6 | 120 mm | Double row | 2.6 ∗ 0.5 ∗ 3 | 17920 | 27249 |
| 7 | 140 mm | Single row | 2.4 ∗ 0.5 ∗ 3 | 15360 | 23763 |
| 8 | 140 mm | Triple flower | 2.66 ∗ 0.5 ∗ 3 | 18240 | 28161 |
| 9 | 140 mm | Double row | 2.66 ∗ 0.5 ∗ 3 | 17920 | 27195 |
| 10 | 160 mm | Single row | 2.44 ∗ 0.5 ∗ 3 | 15360 | 23799 |
| 11 | 160 mm | Triple flower | 2.72 ∗ 0.5 ∗ 3 | 20160 | 31209 |
| 12 | 160 mm | Double row | 2.72 ∗ 0.5 ∗ 3 | 20160 | 31209 |
| 13 | 180 mm | Single row | 2.48 ∗ 0.5 ∗ 3 | 15360 | 23787 |
| 14 | 180 mm | Triple flower | 2.78 ∗ 0.5 ∗ 3 | 20160 | 31179 |
| 15 | 180 mm | Double row | 2.78 ∗ 0.5 ∗ 3 | 23630 | 37777 |
| 16 | 200 mm | Single row | 2.52 ∗ 0.5 ∗ 3 | 15360 | 23799 |
| 17 | 200 mm | Triple flower | 2.84 ∗ 0.5 ∗ 3 | 20160 | 31209 |
| 18 | 200 mm | Double row | 2.84 ∗ 0.5 ∗ 3 | 20160 | 31209 |

Table 2: Mechanical parameters of the coal.

| Elastic modulus (GPa) | Shear modulus (GPa) | Density ($\rho$/kg m$^3$) | Internal friction angle $\psi$ (°) | Tensile strength (MPa) | Cohesive force (MPa) |
|---|---|---|---|---|---|
| 7.1 | 4.3 | 1640 | 30 | 5.6 | 2.1 |

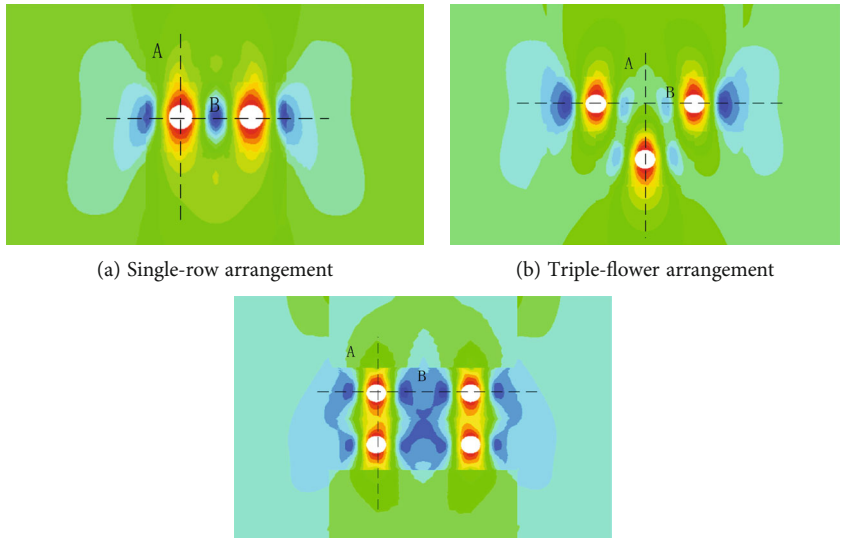


(a) Single-row arrangement

(b) Triple-flower arrangement

(c) Double-row arrangement

Figure 4: Thickness distribution of vertical stress relief zone of the borehole.

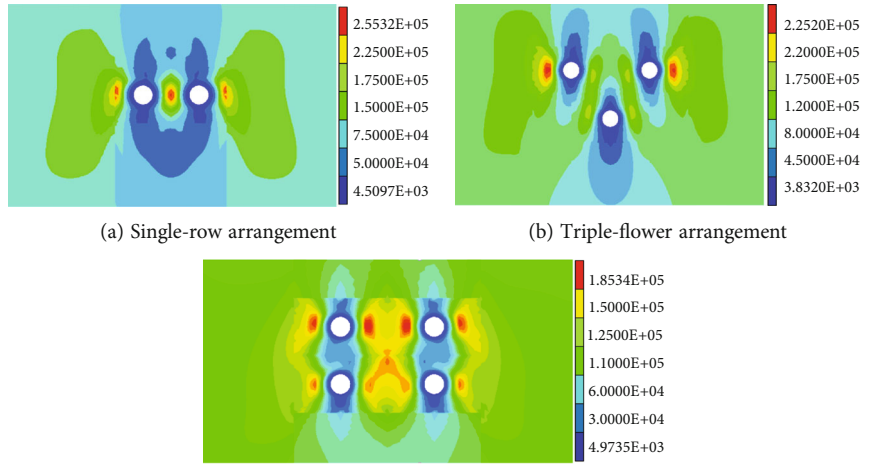


(a) Single-row arrangement (b) Triple-flower arrangement

(c) Double-row arrangement

Figure 5: Energy density distribution in the coal unit.

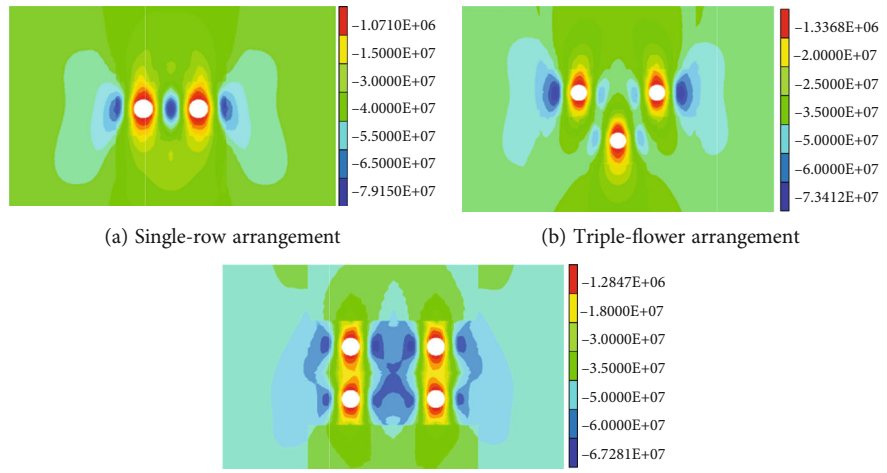


(a) Single-row arrangement (b) Triple-flower arrangement

(c) Double-row arrangement

Figure 6: Vertical stress distribution.

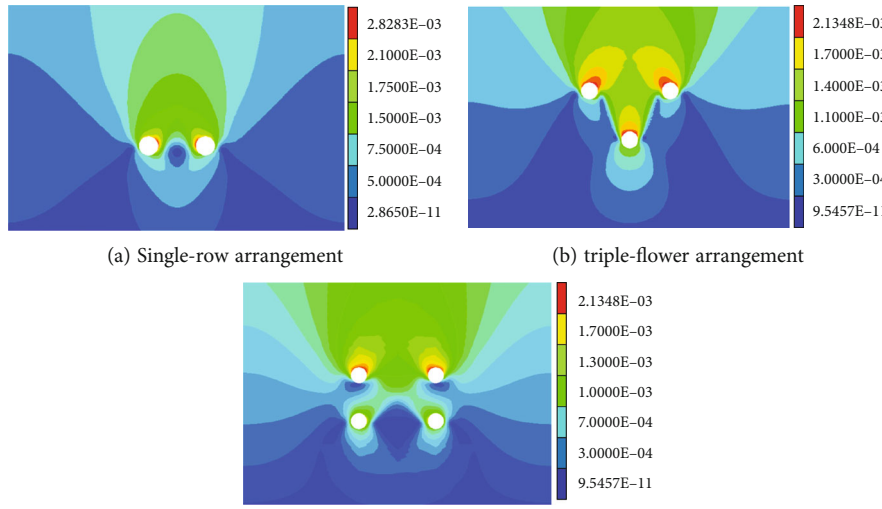


(a) Single-row arrangement (b) triple-flower arrangement

(c) double-row arrangement

Figure 7: Displacement distribution.

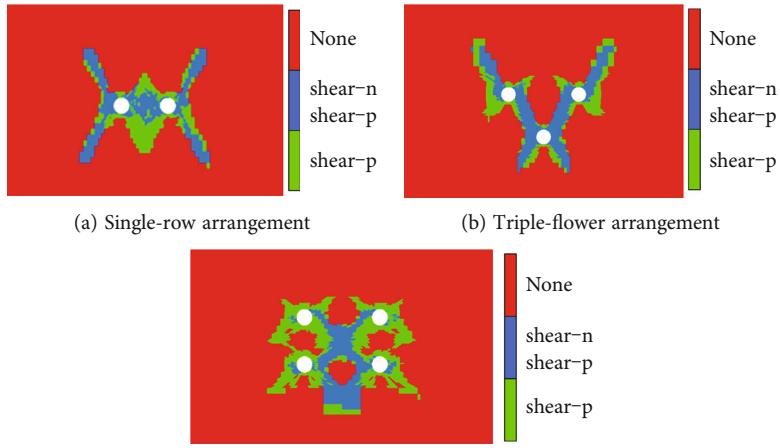


(a) Single-row arrangement (b) Triple-flower arrangement

(c) Double-row arrangement

Figure 8: Distribution of plastic zone.

area at the dotted lines (a) (along the center of the borehole) and (b) (along the center of the borehole spacing) were statistically analyzed. As shown on the figure, when the pressure relief boreholes were arranged in single-row, triple-flower, and double-row forms the thicknesses of the pressure relief areas along the direction of the dotted line in Figure 4(a) were 1, 1.1, and 1.6 m, respectively, and the thickness of the stress concentration area was 0 m. The thicknesses of pressure relief zones along the direction of the dotted line in Figure 4(b) were 0.56, 0.55, and 0.3 m, and those of the stress concentration zone were 0.11, 0.2, and 0.48 m, respectively. The average thickness of the pressure relief zone of the three different arrangements was 0.78, 0.83, and 0.95 m, and that of stress concentration area was 0.11, 0.2, and 0.48 m, respectively.

The above analysis results demonstrate that the thickness of the pressure relief zone was largest in the double-row arrangement, although this led to the thickest stress concentration zone between boreholes. Under the triple-flower arrangement, the thickness of the pressure relief (stress concentration) zone was larger than (similar to) that in the single row. Therefore, the triple-flower arrangement is the best method for relieving the pressure.

*(2) Change in Elastic Energy Density*. Figure 5 shows that the initial elastic energy density of coal is about $1 \times 10^5$ J/m$^3$. After the pressure release by the large-diameter borehole, the minimum elastic energy densities around the borehole were $4.5 \times 10^3$, $3.8 \times 10^3$, and $4.9 \times 10^3$ J/m$^3$ under single-row, triple-flower, and double-row arrangements, respectively. Moreover, the arrangements of single row and double row caused the elastic energy to reaccumulate between boreholes. Therefore, the triple-flower arrangement had the best effect on coal energy release.

*(3) Stress Distribution Law*. Figure 6 shows that the proto-rock stress of the coal seam was about 40 MPa. After the construction of large-diameter pressure relief boreholes,

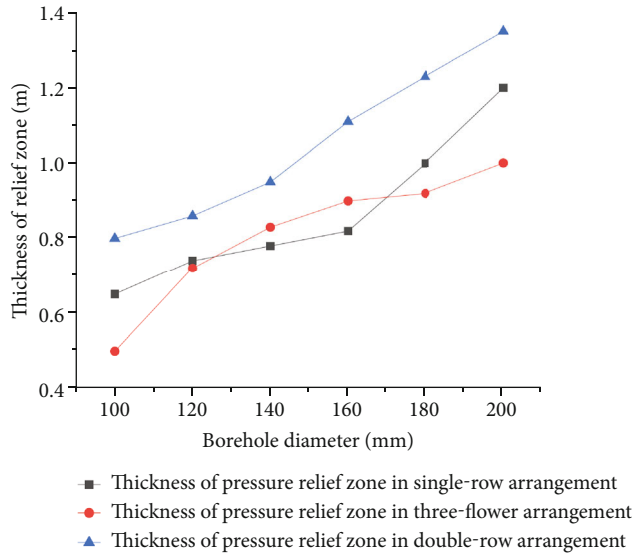


Figure 9: Thickness of pressure relief zone in boreholes with different diameters.

the minimum pressure near the borehole was reduced to about 1, 1.3, and 1.3 MPa under single-row, triple-flower, and double-row arrangements, respectively, and the stress was reduced by about 97%. The three-flowered borehole arrangement resulted in a small stress concentration area between boreholes and smaller stress peak values. Although the stress concentration area between boreholes was also smaller under the single-row arrangement, the peak stress was greater. Moreover, both the stress concentration area and the stress peak value between the boreholes under the double-row arrangement were larger.

*(4) Displacement Law*. Figure 7 shows that the large-diameter pressure relief boreholes under single-row, triple-flower, and double-row arrangements exhibited maximum displacement of $2.8 \times 10^{-3}$, $2.3 \times 10^{-3}$, and $2.1 \times 10^{-3}$ m. It shows that the arrangement of double-row pressure relief

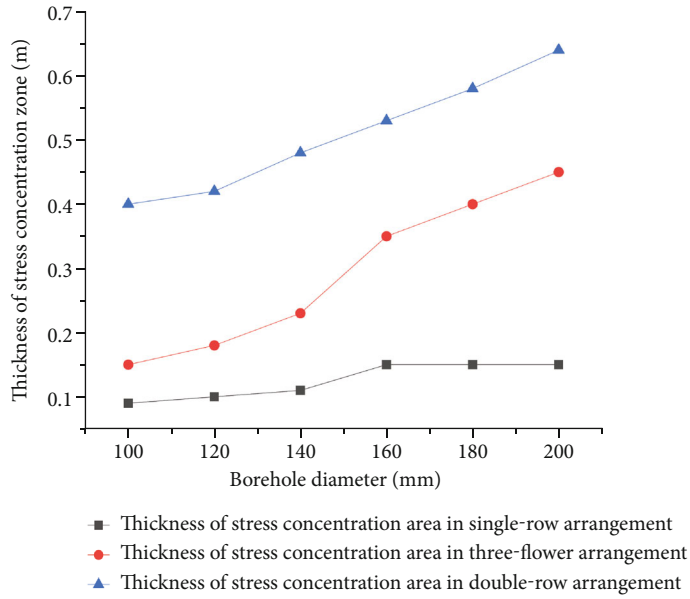


Figure 10: Thickness of stress concentration zone in boreholes with different diameters.

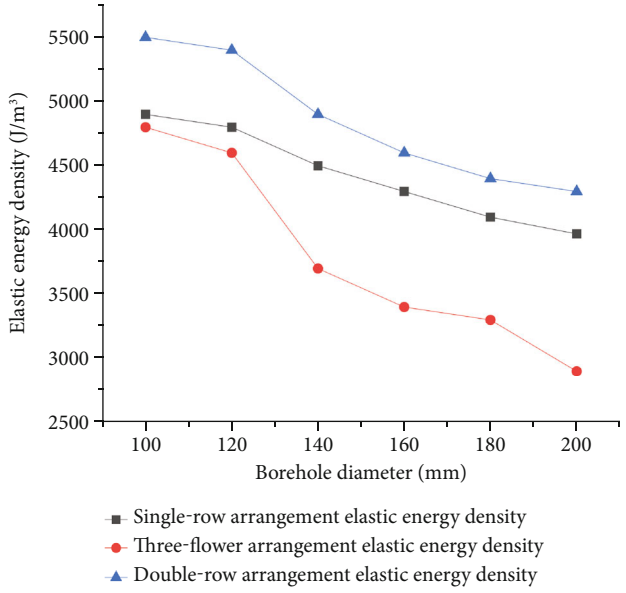


Figure 11: Elastic energy density of boreholes with different diameters.

boreholes has the least impact on the displacement of the coal seam and the effect of controlling the deformation of the roadway is the most significant.

*(5) Plastic Zone Expansion*. Figure 8 shows that under the different arrangements of large-diameter pressure relief boreholes, the plastic zones of the single-row boreholes expanded and penetrated each other, and an effective pressure relief area was formed between the boreholes. Under the three-flower borehole arrangement, the plastic zones between the boreholes were not connected. Under the double-row borehole arrangement, the plastic zone of the diagonally protruding area between the holes was connected but did not penetrate the horizontal interval of the borehole. Thus, under the three-flower and double-row borehole arrangements, the pressure relief effects of the borehole were not ideal.

The above analysis indicates that according to the angles of stress and energy, when the diameter of the pressure relief borehole was 140 mm, although the single-row and double-row borehole arrangements exhibited the best pressure relief effects in the displacement monitoring and the plastic zone, the boreholes were scattered and had less of a coupling effect as well as easy formation of large stress concentration areas, high peak stress, and large elastic energy density accumulation areas between them. Moreover, when the diameter of the pressure relief borehole was 140 mm, the pressure relief effect was the best under the three-flower borehole arrangement.

### *3.2.2. Analysis of the Arrangement of Pressure Relief Boreholes with Different Diameters*

*(1) Thickness of Pressure Relief Zone of Boreholes with Different Diameters*. Figure 9 shows that an increase in the diameter of the pressure relief borehole causes the thickness of the pressure relief zone of the borehole to become significantly larger. In the single-row borehole arrangement, the thickness of the pressure relief zone in the boreholes of 100, 120, 180, and 200 mm in diameter was in the middle of the triple-row and double-row arrangements. In the 140 and 160 mm diameter boreholes, the thickness of the pressure relief zone was in the middle of the single-row and triple-flower arrangements.

*(2) Thickness of Stress Concentration Area of Boreholes with Different Diameters*. Figure 10 shows that as the diameter of the borehole increases, the thickness of the stress

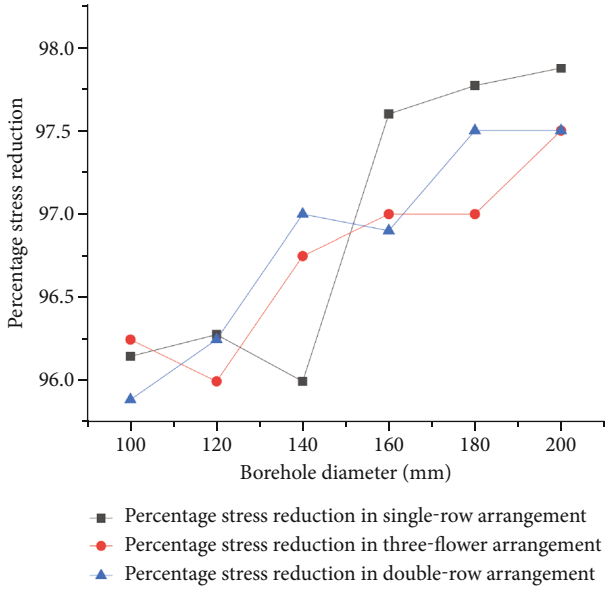


Figure 12: Stress reduction degree in boreholes of different diameter.

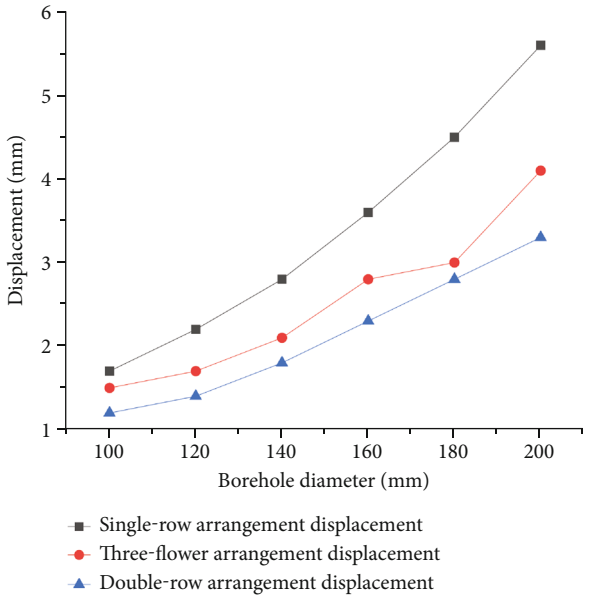


Figure 13: Displacement in boreholes of different diameter.

concentration area also increased, but the thickness of the stress concentration area changed less. In the single-row borehole arrangement, the thickness of the stress concentration area was the smallest. The thickness of the stress concentration area in the three-flower arrangement was in the middle. Under the double-row borehole arrangement, the thickness of the stress concentration area was the largest.

*(3) Changes in Elastic Energy Density of Boreholes with Different Diameters*. Figure 11 shows that the remaining elastic energy density of the coal seam decreased as the diameter of the pressure relief borehole increased. Under the three-flower borehole arrangement, the residual elastic energy density of the coal seam was the smallest. In the single-row borehole arrangement, the residual elastic energy density of the coal seam was in the middle. Under the double-row borehole arrangement mode, the residual elastic energy density of the coal seam was the largest.

Table 3: Plastic zone connection of pressure relief boreholes with different diameters.

| Borehole diameter (mm) | Connection status of the plastic zone of single-row arrangement | Connection status of the plastic zone of three-flower arrangement | Connection status of the plastic zone of double-row arrangement |
|---|---|---|---|
| 100 | y | n | n |
| 120 | y | n | n |
| 140 | y | n | n |
| 160 | y | n | n |
| 180 | y | n | n |
| 200 | y | n | n |

*(4) Stress Distribution Law of Different Diameter Boreholes*. Figure 12 shows that as the borehole diameter increased, the coal seam stress decreased more. For the pressure relief borehole 100 mm in diameter under the three-flower arrangement, the coal seam pressure relief degree was the highest, followed by the single-row arrangement and double-row arrangement. In the pressure relief boreholes with diameters of 120, 180, and 200 mm, under the single-row borehole arrangement, the degree of pressure relief for coal was the highest, followed the double-row arrangement and the three-row arrangement. For pressure relief boreholes 140 and 160 mm in diameter, the degree of pressure relief of the coal seam was in the middle when the three-flower arrangement was used.

*(5) Displacement Law of Boreholes with Different Diameters*. Figure 13 shows that as the borehole diameter increased, the maximum displacement of the coal seam increased. The pressure relief boreholes with different diameters and double-row arrangement had the largest coal displacement. When the three-flower arrangement was used, the coal displacement was the smallest, and the single-row arrangement had middle displacement.

*(6) Expansion Law of Plastic Zone of Different Diameter Boreholes*. Table 3 shows that when the pressure relief boreholes with different diameters were arranged in a single row, the plastic zone was connected. Under the three-flower and double-row arrangements, the plastic zone was not continuously connected; when the double row was arranged, however, the diagonally protruding area between the boreholes was continuously connected.

Based on the above analysis, reasonable arrangement of six types of pressure relief boreholes with different diameters were studied and analyzed. To obtain the final result conveniently and concisely, six indexes were put forward as the

Table 4: Evaluation of the pressure relief effect of different arrangements of pressure relief boreholes with different diameters.

| Evaluation Index | Borehole arrangement | Borehole diameter (mm) | | | | | | | | | | | | | | | | |
|---|---|---|---|---|---|---|---|---|---|---|---|---|---|---|---|---|---|---|
| | | 100 | | | 120 | | | 140 | | | 160 | | | 180 | | | 200 | | |
| | | Single row | Three flower | Double row | Single row | Three flower | Double row | Single row | Three flower | Double row | Single row | Three flower | Double row | Single row | Three flower | Double row | Single row | Three flower | Double row |
| Pressure relief zone thickness | | g | p | e | g | p | e | p | g | e | p | g | e | g | p | e | g | p | e |
| Thickness of stress concentration area | | e | g | p | e | g | p | e | g | p | g | e | p | e | g | p | e | g | p |
| Energy density reduction degree | | g | e | p | g | e | p | g | e | p | g | e | p | g | e | p | g | e | p |
| Stress reduction percentage | | g | e | p | e | p | g | p | g | e | e | g | p | e | p | g | e | g | p |
| Displacement size | | p | g | e | p | g | e | p | g | e | p | g | e | p | g | e | p | g | e |
| Degree of penetration of plastic zone | | e | p | g | e | p | g | e | p | g | e | p | g | e | p | g | e | p | g |

evaluation basis: the average thickness of the pressure relief area (along the dotted lines A and B), the average thickness of the stress concentration area (along the dotted lines A and B), the degree of energy density reduction, the percentage of stress reduction, the size of displacement, and the penetration degree of the plastic zone. Among them, the best, middle, and worst pressure relief result of each index of each diameter borehole was regarded as "excellent," "good," and "poor," respectively. The specific evaluation results are shown in Table 4.

From Table 4, it can be concluded that with borehole diameters of 100, 120, 180, and 200 mm, although the thickness of the stress concentration area was excellent when the boreholes are arranged in a double row, the pressure relief area of the borehole was too small and thus poor. Therefore, the single-row arrangement was optimal. When the borehole diameters were 140 and 160 mm, the arrangement mode under the optimal pressure relief effect of the borehole was the three-flower arrangement. Based on the above analysis, when the diameter of the pressure relief borehole is different, the optimal arrangement of the borehole is also different.

## 4. Theoretical Verification

According to the research results in the literature [34], the pressure relief effects of boreholes were evaluated in the present study under the actual conditions of a mine. To improve the effects of a borehole 200 mm in diameter, three types of borehole arrangement schemes were designed and studied: single-row, three-flower, and square-row arrangements. Through the research and analysis of the thickness and degree of pressure relief area, it was concluded that the proportion of pressure relief area was not different between single-row and three-flower arrangements, although the single-row arrangement showed better effects. In the square-row arrangement, the proportion of the vertical stress concentration area between boreholes was too large owing to the increase in borehole spacing. In terms of the relief effect of vertical stress, the single-row borehole arrangement was the best, followed by the three-flower and square-row arrangements. This is because the boreholes were too scattered, and the mutual coupling effect was small, which can easily form a new stress concentration area.

When the borehole diameter was 200 mm, as shown in Table 4, the single-row borehole arrangement was the optimal solution, which is consistent with the above research results.

## 5. Discussions

In view of the fact that there is no mature theoretical system for the arrangement of pressure relief boreholes with different diameters of single strength coal under high stress conditions, the current design of the arrangement of pressure relief boreholes is mostly determined according to the combination of field experience and national standards. In this paper, under high stress conditions, a reasonable drilling arrangement for pressure relief boreholes with different diameters of a single strength coal seams is proposed. Its advantages and disadvantages are as follows:

(1) By means of theoretical analysis and numerical simulation, the rational layout of different diameter pressure relief boreholes of single strength coal under high stress condition is studied. The basis of reasonable arrangement of pressure relief boreholes with different diameters of single strength coal under high stress condition is put forward. The evaluation table of pressure relief effect of different diameters and different arrangement of pressure relief boreholes is established. The theory of selecting the arrangement of pressure relief boreholes according to the diameter of boreholes is added, which can provide theoretical guidance for determining the reasonable arrangement of pressure relief boreholes with different diameters in coal mine area

(2) In this paper, the object of study only selected the 6 different diameters of pressure drilling, 18 kinds of model is established, the base also is small and is only a preliminary exploration of a theoretical research direction, although it has certain theoretical guiding significance, but whether it has the broad applicability of different intensity of coal, more research is needed; the theory also needs experts further explore perfect

## 6. Conclusion

(1) With an increase in the diameter of the pressure relief borehole, the released elastic energy of the coal near the borehole increased; the residual elastic energy density decreased; the coupling between the boreholes was enhanced; the pressure relief range of the borehole increased; and the pressure relief efficiency was improved

(2) Taking the thicknesses of pressure relief and stress concentration zones as the main evaluation basis and the distribution law of elastic energy density, stress, displacement, and plastic zone after the pressure release of the coal seam as the auxiliary evaluation factors, the pressure relief boreholes with different diameters were examined, and a reasonable borehole arrangement was determined

(3) Six evaluation index systems were proposed to evaluate the pressure relief effect: the thickness of the pressure relief zone, thickness of the stress concentration zone, degree of energy density reduction, percentage of stress reduction, displacement, and penetration degree of the plastic zone. It was determined that when the borehole diameters were 100, 120, 180, and 200 mm, the single-row borehole arrangement had the best pressure relief effect. When the borehole diameters were 140 and 160 mm, the three-flower drilling arrangement was best

(4) It is concluded that pressure relief boreholes with different diameters should adopt different borehole arrangement theories. The results of this research provide a reference basis for setting the optimal pressure relief effect in mining areas according to the actual drilling diameter

## Data Availability

The data that support the study are included in this paper.

## Conflicts of Interest

We declare that we have no conflict of interest.

## Acknowledgments

This paper received financial supports from the National Natural Science Foundation of China (grant numbers: 51674016 and 52004090) and the Natural Science Foundation of Hebei Province (grant number: E2020808025).

## References

[1] J. Yaodong and Z. Yixin, "State of the art: investigation on mechanism, forecast and control of coal bumps in China," *Chinese Journal of Rock Mechanics and Engineering*, vol. 34, no. 11, pp. 2188–2204, 2015.

[2] Q. Qingxin and P. Yongwei, "Study of bursting liability of coal and rock," *Chinese Journal of Rock Mechanics and Engineering*, vol. 30, no. S1, pp. 2736–2742, 2011.

[3] L. M. Dou, J. He, A. Y. Cao, S. Y. Gong, and W. Cai, "Rock burst prevention methods based on theory of dynamic and static combined load induced in coal mine," *Journal of China Coal Society*, vol. 40, no. 7, pp. 1469–1476, 2015.

[4] F. Jiang, G. Yang, and W. Quande, "Study and prospect on coal mine composite dynamic disaster real-time prewarning platform," *Journal of China Coal Society*, vol. 43, no. 2, pp. 333–339, 2018.

[5] J. F. Pan, Y. Ning, D. B. Mao, H. Lan, T. T. Du, and Y. W. Peng, "Theory of rockburst start-up during coal mining," *Chinese Journal of Rock Mechanics and Engineering*, vol. 31, no. 3, pp. 586–596, 2012.

[6] Y. Sun, G. Li, H. Basarir, A. Karrech, and M. R. Azadi, "Laboratory evaluation of shear strength properties for cement-based grouted coal mass," *Arabian Journal of Geosciences*, vol. 12, no. 22, 2019.

[7] Y. Sun, G. Li, N. Zhang, Q. Chang, J. Xu, and J. Zhang, "Development of ensemble learning models to evaluate the strength of coal-grout materials," *International Journal of Mining Science and Technology*, vol. 31, no. 2, pp. 153–162, 2021.

[8] Y. Sun, G. Li, and J. Zhang, "Investigation on jet grouting support strategy for controlling time-dependent deformation in the roadway," *Energy Science & Engineering*, vol. 8, no. 6, pp. 2151–2158, 2020.

[9] Y. D. Jiang, Y. S. Pan, F. X. Jiang, D. O. U. LM, and Y. Ju, "State of the art review on mechanism and prevention of coal bumps in China," *Journal of China Coal Society*, vol. 39, no. 2, pp. 205–213, 2014.

[10] H. Wu, X. Wang, W. Yu et al., "Analysis of influence law of burial depth on surrounding rock deformation of roadway," *Advances in Civil Engineering*, vol. 2020, 13 pages, 2020.

[11] H. Wu, X. Wang, W. Wang, G. Peng, and Z. Zhang, "Deformation characteristics and mechanism of deep subsize coal pillar of the tilted stratum," *Energy Science & Engineering*, vol. 8, no. 2, pp. 544–561, 2020.

[12] L. Dongyin, D. Zhiguo, and L. Zhiyong, "Numerical simulation analysis on parameters of pressure releasing borehole in high stress seam gateway," *Coal Engineering*, vol. 46, no. 9, 2014.

[13] G. Min-min, M. Zhan-guo, G. Peng, and Z. Guo-wei, "Analysis of the effect on pressure relief by the pressure relieving hole layouts in high stress coal roadway," *Journal of Safety Science and Technology*, vol. 8, no. 11, pp. 5–10, 2012.

[14] Y. W. Lan, P. C. Liu, W. Li, X. H. Chen, Z. Y. Lu, and W. Y. Xing, "The influencing factors of drillhole pressure relief and the regression analysis of destroy radius," *Safety in Coal Mines*, vol. 44, no. 4, 2013.

[15] C. Jia, Y. Jiang, X. Zhang, D. Wang, H. Luan, and C. Wang, "Laboratory and numerical experiments on pressure relief mechanism of large-diameter boreholes," *Chinese Journal of Geotechnical Engineering*, vol. 39, no. 6, pp. 1115–1122, 2017.

[16] E. B. Yi, Z. L. Mu, L. M. Dou, J. G. Ju, L. Xie, and D. L. Xu, "Study on comparison and analysis on pressure releasing effect of boreholes in soft and hard seam," *Coal Science and Technology*, vol. 39, no. 6, pp. 1–5, 2011, 85.

[17] W. Meng, W. Xiangyu, and X. Tongqiang, "Borehole destressing mechanism and determination method of its key parameters in deep roadway," *Journal of China Coal Society*, vol. 42, no. 5, pp. 1138–1145, 2017.

[18] H. G. Liu, Y. N. He, J. H. Xu, and L. J. Han, "Numerical simulation and industrial test of boreholes distressing technology in deep coal tunnel," *Journal of China Coal Society*, vol. 32, no. 1, pp. 33–37, 2007.

[19] Z. Hongwei, L. Yunpeng, C. Ying, Z. Feng, and S. Ling-feng, "Research on bumping prevention scheme optimization of large diameter drilling in isolated area under three hard conditions," *Journal of Safety and Environment*, vol. 17, no. 5, pp. 1823–1827, 2017.

[20] Q. Zi-han, "Study of pressure relief with large diameter drilling hole and results verified," *Journal of Mining And Strata Control Engineering*, vol. 23, no. 4, pp. 77–80, 2018.

[21] L. I. Jinkui and X. Zhenhua, "Numerical simulation of borehole pressure relief to prevent rock burst in roadway," *Journal of Xi'an University of Science and Technology*, vol. 29, no. 4, pp. 424–426+432., 2009.

[22] Z. Si-tao, J. Fu-xing, S. Xian-feng et al., "Energy dissipation index method for determining rockburst prevention drilling parameters," *Rock and Soil Mechanics*, vol. 36, no. 8, pp. 2270–2276, 2015.

[23] S. Qing-wen, C. Hong-ke, L. Da-zhao, P. Jun-feng, X. Yong-xue, and W. Shu-wen, "Study on pressure relief drilling holes layout parameters of roadside in rockburst coal seam," *Journal of Mining And Strata Control Engineering*, vol. 22, no. 6, pp. 74–77, 2017.

[24] D. Li, F. X. Jiang, Y. Chen, D. C. Gai, Y. Wang, and W. B. Wang, "Study on impact mechanism and prevention technology of drainage lane of large coal pillars near deep wells," *Journal of Mining & Safety Engineering*, vol. 36, no. 2, pp. 265–271, 2019.

[25] W. Shu-wen, P. Jun-feng, L. Shao-hong, X. Yong-xue, Y. Lei, and G. Xiao-jin, "Evaluation method for rockburst-preventing effects by drilling based on energy-dissipating rate," *Journal of China Coal Society*, vol. 41, no. S2, pp. 297–304, 2016.

[26] C. Zhai, J. Xu, S. Liu, and L. Qin, "Investigation of the discharge law for drill cuttings used for coal outburst prediction based on different borehole diameters under various side stresses," *Powder Technology*, vol. 325, pp. 396–404, 2018.

[27] Y. Li, H. W. Zhang, J. Han, F. Zhu, and C. Guo, "Time effect of borehole pressure relief based on distributed optical fiber sensing technology," *Journal of China Coal Society*, vol. 42, no. 11, pp. 2834–2841, 2017.

[28] S. Zhang, Y. Li, B. Shen, X. Sun, and L. Gao, "Effective evaluation of pressure relief drilling for reducing rock bursts and its application in underground coal mines," *International Journal of Rock Mechanics and Mining Sciences*, vol. 114, pp. 7–16, 2019.

[29] D. Ge, D. Li, and F. Jiang, "Reasonable pressure-relief borehole spacing in coal of different strength," *Journal of Mining & Safety Engineering*, vol. 37, no. 3, pp. 578–585, 2020.

[30] G. Yong-ge, J. Zhi-xin, M. Xiao-qiang, and Z. Ji-yun, "Effects of hole diameter and arrangement on tunneling surface relief effect," *Coal Technology*, vol. 36, no. 1, pp. 138–140, 2017.

[31] X. Heping, J. Yang, and L. Liyun, "Criteria for strength and structural failure of rocks based on energy dissipation and energy release principles," *Chinese Journal of Rock Mechanics and Engineering*, vol. 24, no. 17, pp. 3003–3010, 2005.

[32] R. Solecki and R. J. Conant, *Advanced mechanics of materials*, Oxford University Press, London, 2003.

[33] G. S. Su, X. T. Feng, Q. Jiang, and G. Q. Chen, "Study on new index of local energy release rate for stability analysis and optimal design of underground rockmass engineering with high geostress," *Chinese Journal of Rock Mechanics and Engineering*, vol. 25, no. 12, pp. 2453–2460, 2006.

[34] W. Shuwen, M. Debing, and R. Yong, "Parameter optimizating of drilling holes for pressure relief," *Journal of Mining And Strata Control Engineering*, vol. 15, no. 5, pp. 14–17, 2010.